# Dynamic theory of correlations in strongly coupled, classical one-component plasmas: Glass transition in the generalized viscoelastic formalism

Shigenori Tanaka and Setsuo Ichimaru
*Department of Physics, University of Tokyo, 7-3-1 Hongo, Bunkyo-ku, Tokyo 113, Japan*
(Received 15 December 1986)

A new theory of dynamic correlations in a strongly coupled, classical one-component plasma (OCP) is developed within the generalized viscoelastic formalism. Fully convergent kinetic equations for the strongly coupled OCP are thereby derived with the aid of a fluctuation-theoretic formulation of the collision integrals. The dynamic structure factor $S(k,\omega)$ and the coefficient $\eta$ of shear viscosity are calculated both in the ordinary fluid state and in the metastable supercooled state through a self-consistent solution to the kinetic equation. It is shown that the numerical results in the ordinary fluid state agree well with other theoretical and molecular-dynamics simulation results. A possibility of the dynamic glass transition is predicted in the supercooled OCP through the analyses of the variation in $\eta$, the quasielastic peak in $S(k,\omega)$ and the behavior of the self-diffusion coefficient; the prediction is compared with those in the glass-transition theories for other systems. Relevance to laboratory experiment is examined in terms of the metastable-state lifetimes against homogeneous nucleation of the crystalline state.

## I. INTRODUCTION

The classical one-component plasma (OCP) consisting of a single species of point charges (electric charge $Ze$, mass $m$, number density $n$, and temperature $T$) embedded in a uniform background of neutralizing charges represents one of the well-studied, nontrivial statistical systems.[1,2] The state of an OCP system is characterized by a single dimensionless Coulomb-coupling constant,

$$\Gamma=(Ze)^2/ak_BT\ , \tag{1}$$

where $a=(4\pi n/3)^{-1/3}$ is the Wigner-Seitz (ion-sphere) radius.

The static and dynamic properties of a strongly coupled OCP such that $\Gamma\gg 1$ differs markedly from those of a weakly coupled OCP, $\Gamma\ll 1$. The correlation properties of such a strongly coupled OCP have been extensively studied by the Monte Carlo (MC) and molecular-dynamics (MD) simulation techniques[3-5] as well as by numerical solutions to integral equations.[6-8] Practically, it provides a workable model for dense stellar matter such as those found in the interior of a degenerate star and in the outer crust of a neutron star;[9] recent experimental developments[10,11] lead us to expect that a strongly coupled OCP may soon be realized in a laboratory setting.

It has been shown[3] through the MC experiments that the OCP may undergo a phase transition into a crystalline state (Wigner crystallization) at the critical $\Gamma$ value, $\Gamma_m=178\pm 1$. Since the transition is of the first order, the plasma may remain in a metastable fluidlike state when it is supercooled below the corresponding transition temperature; astrophysical implications of taking account of such a supercooled fluid plasma have been discussed elsewhere.[12] If such a plasma is quenched sufficiently rapidly to overcome a homogeneous nucleation of crystalline lattices, the plasma may possibly turn into a glassy state.[13,14]

Recently, the MC and MD experiments for the supercooled simple liquids have been extensively carried out;[13-16] the possibilities of the glass transition in systems such as the hard-sphere (HS), the soft-sphere, and the Lennard-Jones (LJ) have been thereby elucidated. Theoretical accounts of the computer-simulation results were also made by a number of investigators on the basis of a self-consistent mode-coupling theory[17,18] or a nonlinear fluctuating hydrodynamic theory.[19]

We remark in this connection that the OCP system may offer a unique object of study, in that it is probably a most difficult system to make a glass; the point charges, interacting via one of the softest and symmetric binary potentials, may be viewed as too "elusive" to lock themselves into a glassy state. On the other hand, we recall the similarity between the strongly coupled OCP and the HS system demonstrated in various physical cases;[2,6,20,21] this similarity may act to enhance the possibility of a glass transition. In light of both the theoretical significance and the practical feasibility of the experimental study, we thus find it important to clarify the nature of the OCP in the supercooled state and to explore the possibility of a glass transition.

In this paper we present a new theory of dynamic correlations for the strongly coupled OCP within the generalized viscoelastic formalism[22] coupled with a kinetic theory; the theory reproduces the existing MD simulation data for $\Gamma<\Gamma_m$ both on the dynamic structure factor[4] $S(k,\omega)$ and on the coefficient of shear viscosity[5] $\eta$ satisfactorily. We then extend the theory to those plasmas in the supercooled state, $\Gamma>\Gamma_m$, investigate the dynamic behaviors of the system, and analyze the possibility of a glass transition.

In Sec. II the static properties of the supercooled OCP are investigated through analyses of the radial distribution function $g(r)$ and the static structure factor $S(k)$ calcu-

 

lated on the basis of the improved hypernetted chain (IHNC) scheme;[7] delicate changes observed in the correlation functions are interpreted as precursors of a dynamic glass transition which will take place at a still larger value of $\Gamma$. In Sec. III we formulate a dynamic theory in which the viscoelastic theory on the OCP is generalized into finite frequency and wave-number regimes, and construct the dynamic local-field correction $G(k,\omega)$ describing the strong Coulomb-coupling effects. The coefficient of shear viscosity $\eta$ appearing in the expression for $G(k,\omega)$ is then calculated in Sec. IV through a solution to the kinetic equation, whose collision term in turn is expressed by $G(k,\omega)$; we thus determine $\eta$ and $G(k,\omega)$ self-consistently. The numerical results for $\eta$ and $S(k,\omega)$ are presented in Sec. V; the self-diffusion coefficient $D$ is estimated by assuming the correspondence between the OCP and HS systems. The possibility of a glass transition at $\Gamma\simeq 1000$ will be revealed in the dynamic properties through the variation of $\eta$. In Sec. VI the lifetime of a metastable fluid state against a homogeneous nucleation of crystals is evaluated according to a standard statistical model; the rate of rapid quench necessary for the formation of a glass is estimated and the experimental possibilities are assessed. Summary and concluding remarks are given in Sec. VII.

A preliminary account of the present work has been reported elsewhere.[23]

## II. STATIC PROPERTIES

In this section we investigate the static properties of the correlations in the supercooled OCP. The static correlation functions such as $g(r)$ and $S(k)$ not only are necessary as inputs to calculate the dynamic correlation functions but also give some information on the structural changes associated with the glass transition.

We calculate the static correlation functions with the improved hypernetted-chain (IHNC) scheme of Iyetoni and Ichimaru,[7] in which the contribution of the bridge diagrams neglected in the hypernetted-chain (HNC) approximation are taken into account appropriately. It has been confirmed[7] that the IHNC scheme almost identically reproduces the existing MC data[3] of $g(r)$ for $\Gamma \leq 160$; the excess internal energies agree with the MC values with digressions less than 0.14%.

In Fig. 1 we exhibit the results for $g(r)$ calculated by extending the IHNC scheme to those plasmas in the supercooled state. The most striking features[12] in the IHNC solution are the broadening (at $\Gamma\approx 200$) and the subsequent splitting into two parts (for $\Gamma \gtrsim 300$) of the second peak in $g(r)$. We clearly observe such a splitting of the second peak and structural developments around the third peak in Fig. 1 as $\Gamma$ increases to and beyond 500. We add a parenthetical remark that those features in $g(r)$ have not arisen as an artifact of the IHNC scheme; even an inclusion of only the lowest-order bridge-diagram contribution leads to the split-second-peak structures for $\Gamma \gtrsim 400$.

We have also computed the Wendt-Abraham ratio[24] $\mathscr{R}\equiv g_{\min}/g_{\max}$ between the first minimum and maximum in $g(r)$ for various $\Gamma$ values; the results are plotted in Fig. 2. We find that $\mathscr{R}$ has a power-law dependence on $\Gamma$ and

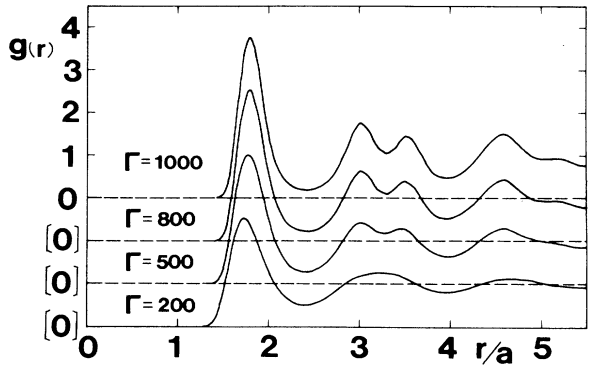


FIG. 1. Radial distribution function of the supercooled OCP computed in the IHNC scheme at various values of $\Gamma$.

that the index changes approximately from $-0.7$ to $-0.9$ somewhere between $\Gamma=300$ and 400. The point at which the two asymptotic lines intersect is $\Gamma\simeq 330$ and $\mathscr{R}\simeq 0.14$; the former appears to correlate with the splitting of the second peak in $g(r)$ and the latter coincides exactly with the empirical value originally found by Wendt and Abraham[24] through the analyses of the MC data for the 12-6 LJ system.

A number of differences between the OCP and LJ systems are to be noted in this regard, however. First, $\mathscr{R}$ exhibits a linear dependence on $T$, whose slope changes at the transition point, in the LJ case. Second, the observed kink is concave in the LJ system, contrary to the OCP cases as depicted in Fig. 2. Finally, we remark that the characteristic volume also displays an analogous kink as a function of $T$ in the LJ system, while the characteristic volume in the OCP is consistent by definition.

The IHNC results for the static structure factor $S(k)$ are also shown in Fig. 3; we observe structural developments quite analogous to Fig. 1.

For the supercooled OCP to be in a metastable state, it must be stable against the onset of a soft-mode instability of the charge-density-wave (CDW) type. The onset condition[25] for the CDW instability has been investigated in

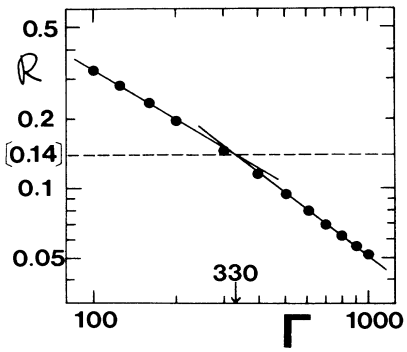


FIG. 2. Wendt-Abraham ratio $\mathscr{R}\equiv g_{\min}/g_{\max}$ vs the coupling constant $\Gamma$. Two asymptotic straight lines represent power-law fittings of $\mathscr{R}$ on $\Gamma$. The horizontal dashed line refers to $\mathscr{R}=0.14$.

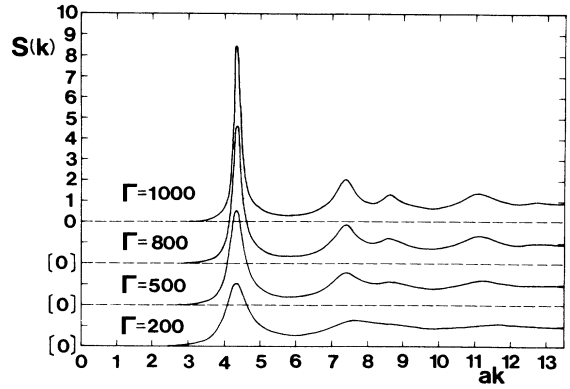


FIG. 3. Static structure factor of the supercooled OCP computed in the IHNC scheme at various values of Γ.

terms of the IHNC results for $S(k)$. It has thereby been found that the metastability of the fluid phase may persist beyond $\Gamma=1000$, up to a substantially large $\Gamma$ value.

Although the structural developments observed above in $g(r)$ and $S(k)$ may be interpreted as indications of a glass transition in the OCP system, their appearance is quite a delicate affair and is not universal in dense systems.[13] We rather take a point of view that the glass transition is basically a dynamic phenomenon and that the features in the static structures are to be regarded as precursors suggesting a possibility of the dynamic glass transition. We therefore proceed to investigate the dynamic properties of the strongly coupled OCP in the following sections.

## III. DYNAMIC LOCAL-FIELD CORRECTION BASED ON GENERALIZED VISCOELASTIC FORMALISM

The strong Coulomb-coupling effects are described in the present theory through the dynamic local-field correction (DLFC) $G(k,\omega)$, which is introduced via the wave vector $\mathbf{k}$ and frequency $\omega$ dependent linear-response relation between the external potential $\varphi_{\rm ext}(\mathbf{k},\omega)$ and the induced density fluctuations $\delta n(\mathbf{k},\omega)$,[2,26]

$$\delta n(\mathbf{k},\omega)=\chi_0(\mathbf{k},\omega)\{\varphi_{\rm ext}(\mathbf{k},\omega)+v(k)[1-G(k,\omega)]\delta n(\mathbf{k},\omega)\} . \tag{2}$$

Here $v(k)=4\pi(Ze)^2/k^2$ and $\chi_0(\mathbf{k},\omega)$ is the retarded free-particle polarizability,

$$\chi_0(\mathbf{k},\omega)=-\int d\mathbf{p}\frac{1}{\omega-\mathbf{k}\cdot\mathbf{v}+i0}\mathbf{k}\cdot\frac{\partial F}{\partial\mathbf{p}} , \tag{3}$$

where 0 in the denominator denotes a positive infinitesimal. In the equilibrium system, the single-particle distribution function $F=F(X;t)$ is Maxwellian,

$$F_0(p)=n\left[\frac{1}{2\pi mk_BT}\right]^{3/2}\exp\left[-\frac{p^2}{2mk_BT}\right] , \tag{4}$$

where $X\equiv(\mathbf{r},\mathbf{p})$ and $\mathbf{p}=m\mathbf{v}$.

The dielectric response function of the OCP is expressed by $G(k,\omega)$ as

$$\epsilon(k,\omega)=1-\frac{v(k)\chi_0(k,\omega)}{1+v(k)G(k,\omega)\chi_0(k,\omega)} . \tag{5}$$

The dynamic structure factor can be calculated with the knowledge of $\epsilon(k,\omega)$ via the fluctuation-dissipation theorem[27] as

$$S(k,\omega)=-\frac{k_BT}{\pi v(k)\omega}\mathrm{Im}\frac{1}{\epsilon(k,\omega)} . \tag{6}$$

The static structure factor is then given by[27]

$$S(k)=\frac{1}{n}\int_{-\infty}^{\infty}d\omega S(k,\omega)=\frac{k^2}{k^2+k_D^2[1-G(k)]} , \tag{7}$$

where $k_D=[4\pi n(Ze)^2/k_BT]^{1/2}$ and $G(k)\equiv G(k,\omega=0)$ is the static local-field correction (SLFC).[2]

In order to obtain the DLFC, we evoke the linearized viscoelastic equations of motion[22] for the OCP,

$$\frac{\partial}{\partial t}\delta n(\mathbf{r},t)+n\frac{\partial}{\partial\mathbf{r}}\cdot\delta\mathbf{u}(\mathbf{r},t)=0 , \tag{8}$$

$$mn\frac{\partial}{\partial t}\delta\mathbf{u}(\mathbf{r},t)=-\frac{\partial}{\partial\mathbf{r}}\Pi(\mathbf{r},t) , \tag{9}$$

$$\left[1+\tau_m\frac{\partial}{\partial t}\right]\left[\frac{\partial}{\partial\mathbf{r}}\Pi(\mathbf{r},t)-\frac{\partial}{\partial\mathbf{r}}P(\mathbf{r},t)+Ze n\mathbf{E}(\mathbf{r},t)\right]=-\eta\frac{\partial}{\partial\mathbf{r}}\cdot\frac{\partial}{\partial\mathbf{r}}\delta\mathbf{u}(\mathbf{r},t)-\left[\zeta+\frac{\eta}{3}\right]\frac{\partial}{\partial\mathbf{r}}\frac{\partial}{\partial\mathbf{r}}\cdot\delta\mathbf{u}(\mathbf{r},t) , \tag{10}$$

$$nT\frac{\partial}{\partial t}\delta s(\mathbf{r},t)=\kappa\frac{\partial}{\partial\mathbf{r}}\cdot\frac{\partial}{\partial\mathbf{r}}\delta T(\mathbf{r},t) . \tag{11}$$

Here the fluctuating quantities, $\delta\mathbf{u}$, $\Pi$, $P$, $\mathbf{E}$, $\delta s$, and $\delta T$, represent the flow velocity, the isotropic part of the momentum flow tensor, the pressure, the electric field, the entropy and the temperature, respectively; $\tau_m$, $\zeta$, and $\kappa$ are the viscoelastic relaxation time, the bulk viscosity and the thermal conductivity. If $\tau_m$ is set equal to zero in Eq. (10), one recovers the Navier-Stokes equation in the case of OCP.[28]

We shall consider the isothermal response so that $\delta T=0$. According to the density-response formalism,[26] we apply to the system a weak external potential field $\varphi_{\rm ext}(\mathbf{k},\omega)$. Fourier transforming Eqs. (8)—(10) and noting the Poisson equation,

$$\mathbf{E}(\mathbf{k},\omega)=-i\mathbf{k}\left[\varphi_{\rm ext}(\mathbf{k},\omega)+\frac{v(k)}{Ze}\delta n(\mathbf{k},\omega)\right] , \tag{12}$$

we obtain

$$\delta n(\mathbf{k},\omega)=Ze\chi_v(k,\omega)\varphi_{\rm ext}(\mathbf{k},\omega) . \tag{13}$$

Here

$$\chi_v(k,\omega)=\frac{n}{m}\left[\frac{k}{\omega}\right]^2\Big/\left[1+i\frac{\eta_l(\omega)}{mn}\frac{k^2}{\omega}-\frac{1}{m}\left[\frac{\partial P}{\partial n}\right]_T\left[\frac{k}{\omega}\right]^2-\left[\frac{\omega_p}{\omega}\right]^2\right] \tag{14}$$

is the density response function in the viscoelastic formalism, $\eta_l(\omega)=\eta_l/(1-i\omega\tau_m)$, $\eta_l=\frac{4}{3}\eta+\zeta$, and $\omega_p=[4\pi n(Ze)^2/m]^{1/2}$. We thus find an isothermal dielectric response function

$$\epsilon_v(k,\omega)=1-\frac{v(k)\chi_{v0}(k,\omega)}{1+v(k)G_v(k,\omega)\chi_{v0}(k,\omega)}\ , \tag{15}$$

where

$$\chi_{v0}(k,\omega)=\frac{n}{m}\left[\frac{k}{\omega}\right]^2\Big/\left[1-\frac{k_BT}{m}\left[\frac{k}{\omega}\right]^2\right]\ , \tag{16}$$

and

$$G_v(k,\omega)=\frac{k^2}{k_D^2}\left[1-\frac{1}{k_BT}\left[\frac{\partial P}{\partial n}\right]_T+\frac{i\omega}{nk_BT}\eta_l(\omega)\right] \tag{17}$$

is the DLFC in the viscoelastic formalism. In the ensuing calculations, we shall ignore $\zeta$ and approximate the longitudinal viscosity $\eta_l=\frac{4}{3}\eta$; it has been found[5,28] that $\zeta$ is negligible compared to $\eta$ in the OCP.

We now generalize the viscoelastic dielectric function $\epsilon_v(k,\omega)$ into a finite $k$ and $\omega$ regime, so that $\eta_l(k)$ and $\tau_m(k)$ are functions of $k$. First, a straightforward generalization of the free-particle polarizability, $\chi_{v0}(k,\omega)\to\chi_0(k,\omega)$, Eq. (3), is performed. Noting that the viscoelastic SLFC $G_v(k)=G_v(k,0)$ satisfies the compressibility sum rule,[1,2] we generalize

$$G_v(k)\to G(k)=1+\frac{k^2}{k_D^2}\left[1-\frac{1}{S(k)}\right]\ . \tag{18}$$

In light of the third frequency-moment sum rule[1,2] we may then set

$$G_v(k,\infty)\to I(k) \tag{19}$$

with

$$I(k)=\frac{1}{n}\int\frac{d\mathbf{q}}{(2\pi)^3}\left[\frac{\mathbf{k}\cdot\mathbf{q}}{q^2}+\frac{\mathbf{k}\cdot(\mathbf{k}-\mathbf{q})}{|\mathbf{k}-\mathbf{q}|^2}\right]\frac{\mathbf{k}\cdot\mathbf{q}}{k^2}\times[1-S(|\mathbf{k}-\mathbf{q}|)]\ . \tag{20}$$

From Eqs. (17)–(19) we obtain

$$\eta_l(k)/\tau_m(k)=nk_BT(k_D/k)^2[G(k)-I(k)]\ . \tag{21}$$

Substitution of Eqs. (18) and (21) in Eq. (17) yields

$$G_v(k,\omega)\to G(k,\omega)=\frac{G(k)-i\omega\tau_m(k)I(k)}{1-i\omega\tau_m(k)}\ , \tag{22}$$

and $\epsilon_v(k,\omega)\to\epsilon(k,\omega)$, Eq. (5). The DLFC as expressed in Eq. (22) has a form in which the low-frequency limit $G(k)$ and the high-frequency limit $I(k)$ are interpolated through an exponential damping function;[26,29] $\tau_m(k)$ plays the role of the characteristic time distinguishing between the low- and high-frequency regimes.

For a hydrodynamic mode, where we are concerned only with low-frequency and long-wavelength excitations, the first term, unity, on the right-hand side of Eq. (5) is negligible, since $|v(k)\chi_0(k,\omega)|\gg 1$. We thus find the quasielastic peak in the dynamic structure factor from Eqs. (5), (6), and (22),

$$S(k,\omega)\simeq\frac{n}{\pi}\left[\frac{k}{k_D}\right]^2\frac{\tau_m(k)}{1+[\omega\tau_m(k)]^2}[G(k)-I(k)]\ . \tag{23}$$

In the limit of $\tau_m(k)\to\infty$,

$$S(k,\omega)\to n(k/k_D)^2[G(k)-I(k)]\delta(\omega)\ . \tag{24}$$

This limit thus corresponds to a frozen state[17,18] in which the local structure does not vanish even after an infinite time or the expectation value $\langle\delta n(\mathbf{k},t)\delta n^*(\mathbf{k},0)\rangle$ stays finite for $t=\infty$; these features point to a dynamic transition to a glassy state.

In the long-wavelength limit we have

$$\tau_m(0)=\frac{\eta_l}{nk_BT}\Big/\left[1-\frac{1}{k_BT}\left[\frac{\partial P}{\partial n}\right]_T+\frac{4}{15}u_{\rm ex}\right] \tag{25}$$

from Eq. (21) where $u_{\rm ex}$ refers to the excess internal energy density divided by $nk_BT$. When the relaxation time is written as

$$\tau_m(k)=\tau_m(0)Y(k) \tag{26}$$

with $Y(0)=1$, $Y(k)$ remains the only function to be determined.

The viscoelastic relaxation time $\tau_m(k)$ has been introduced to remove a certain rigidity inherent in the Navier-Stokes equation with regard to temporal response of the internal energy against the viscous motion of the fluid. Without the relaxation effect, the viscous motion cannot be made compatible with the third frequency-moment sum rule or with the quasielastic peak. Let us also recall the cage effect in dense liquid,[18] where a single particle has a tendency to be trapped by the surrounding particles; to simulate this effect, we expect the inverse Fourier transform of $\tau_m(k)$ to be a real function in the $r$ space. In addition, the relaxation time $\tau_m(k)$ must be a positive-definite quantity for reasons of causality and should vanish as the size ($\sim k^{-1}$) of the fluctuation tends to zero.

Taking the aforementioned conditions into consideration, we adopt two forms for $Y(k)$; a Gaussian approximation,

$$Y_G(k)=\exp[-(ak/\xi_G)^2]\ , \tag{27}$$

and a Lorentzian approximation,

$$Y_L(k)=[1+(ak/\xi_L)^2]^{-1}\ , \tag{28}$$

where $\xi_G$ and $\xi_L$ take on values of order unity. The free

parameters $\xi_G$ and $\xi_L$ are assumed to be independent of $\Gamma$ and are adjusted so that the resulting values of $\eta$ appropriately reproduce the existing MD results[1,5] for $\Gamma \leq 100$. The computational details for determination of $\xi$ shall be described in Sec. V.

## IV. CONVERGENT COLLISION TERM AND SHEAR VISCOSITY

In Sec. III we have derived an expression for $G(k,\omega)$ in the framework of the generalized viscoelastic formalism; the coefficient $\eta$ of shear viscosity remains to be determined in the expression. In this section we develop a kinetic equation and solve it to obtain an explicit expression for $\eta$ in terms of $G(k,\omega)$. We thus establish a self-consistent scheme to calculate $\eta$ and $G(k,\omega)$ simultaneously.

For a description of a nonequilibrium system, we begin with an exact kinetic equation,

$$\frac{\partial F}{\partial t}+\mathbf{v}\cdot\frac{\partial F}{\partial \mathbf{r}}+Ze\left[\mathbf{E}+\frac{\mathbf{v}}{c}\times\mathbf{B}\right]\cdot\frac{\partial F}{\partial \mathbf{p}}=\left.\frac{\partial F}{\partial t}\right|_c , \tag{29}$$

where the collision term for the system of charged particles is expressed as

$$\left.\frac{\partial F}{\partial t}\right|_c=-iZe\int\frac{d\mathbf{k}}{(2\pi)^3}\int d\omega\,\mathbf{k}\cdot\frac{\partial}{\partial \mathbf{p}}\langle\delta N\,\varphi^*(\mathbf{k},\omega;\mathbf{p})\rangle . \tag{30}$$

Here $\delta N(\mathbf{k},\omega;\mathbf{p})$ and $\varphi(\mathbf{k},\omega)$ refer to the microscopic density fluctuations and the potential fluctuations, respectively; the angular brackets denote the spectral function.[9]

We may separate $\delta N(\mathbf{k},\omega;\mathbf{p})$ into two parts: the spontaneous fluctuations and the induced fluctuations, as[9,30,31]

$$\delta N(\mathbf{k},\omega;\mathbf{p})=\delta N_0(\mathbf{k},\omega;\mathbf{p})+\delta N_s(\mathbf{k},\omega;\mathbf{p}) . \tag{31}$$

Extending the idea of the static polarization-potential model of density fluctuations[26,30–32] to the dynamic case, we may express the induced part as

$$\delta N_s(\mathbf{k},\omega;\mathbf{p})=-Ze\mathbf{k}\cdot\frac{\partial F}{\partial \mathbf{p}}\frac{\varphi(\mathbf{k},\omega)}{\omega-\mathbf{k}\cdot\mathbf{v}+i0}[1-G(\mathbf{k},\omega)] . \tag{32}$$

In this expression the strong (nonlinear) Coulomb-coupling effects between density fluctuations which go beyond the Born approximation have been taken into account through the DLFC given by Eq. (22). In reference to Eq. (2) and the Poisson equation

$$\varphi(\mathbf{k},\omega)=\frac{v(k)}{Ze}\delta n(\mathbf{k},\omega) \tag{33}$$

with

$$\delta n(\mathbf{k},\omega)=\int d\mathbf{p}\,\delta N(\mathbf{k},\omega;\mathbf{p}) , \tag{34}$$

we may regard the spontaneous part $\delta N_0(\mathbf{k},\omega;\mathbf{p})$ as a sort of external field in Eqs. (31) and (32).

From Eqs. (31)–(33) we express $\delta n(\mathbf{k},\omega)$ as

$$\delta n(\mathbf{k},\omega)=\frac{\delta n_0(\mathbf{k},\omega)}{\tilde{\epsilon}(\mathbf{k},\omega)} , \tag{35}$$

where

$$\tilde{\epsilon}(\mathbf{k},\omega)=1-v(k)[1-G(k,\omega)]\chi_0(\mathbf{k},\omega) \tag{36}$$

and

$$\delta n_0(\mathbf{k},\omega)=\int d\mathbf{p}\,\delta N_0(\mathbf{k},\omega;\mathbf{p}) . \tag{37}$$

Substituting Eqs. (31)–(33) in Eq. (30) and noting that[9,30]

$$\langle\delta N_0(\mathbf{k},\omega;\mathbf{p})\delta n_0^*(\mathbf{k},\omega)\rangle=F(\mathbf{p})\delta(\omega-\mathbf{k}\cdot\mathbf{v}) , \tag{38}$$

we finally obtain

$$\left.\frac{\partial F}{\partial t}\right|_c=C_R+C_I \tag{39}$$

with

$$C_R=\pi\int\frac{d\mathbf{k}}{(2\pi)^3}\mathbf{k}\cdot\frac{\partial}{\partial \mathbf{p}}\int d\mathbf{p}'\frac{v(k)^2[1-\mathrm{Re}G(k,\mathbf{k}\cdot\mathbf{v})]}{|\tilde{\epsilon}(k,\mathbf{k}\cdot\mathbf{v})|^2}\times\delta(\mathbf{k}\cdot\mathbf{v}-\mathbf{k}\cdot\mathbf{v}')\mathbf{k}\cdot\left[\frac{\partial}{\partial \mathbf{p}}-\frac{\partial}{\partial \mathbf{p}'}\right]\times F(\mathbf{p})F(\mathbf{p}') \tag{40}$$

and

$$C_I=\int\frac{d\mathbf{k}}{(2\pi)^3}\mathbf{k}\cdot\frac{\partial}{\partial \mathbf{p}}\int d\mathbf{p}'[v(k)]^2\mathrm{P}\frac{1}{\mathbf{k}\cdot\mathbf{v}'-\mathbf{k}\cdot\mathbf{v}}\left[\frac{\mathrm{Im}G(k,\mathbf{k}\cdot\mathbf{v}')}{|\tilde{\epsilon}(k,\mathbf{k}\cdot\mathbf{v}')|^2}\mathbf{k}\cdot\frac{\partial}{\partial \mathbf{p}}+\frac{\mathrm{Im}G(k,\mathbf{k}\cdot\mathbf{v})}{|\tilde{\epsilon}(k,\mathbf{k}\cdot\mathbf{v})|^2}\mathbf{k}\cdot\frac{\partial}{\partial \mathbf{p}'}\right]F(\mathbf{p})F(\mathbf{p}') , \tag{41}$$

where P stands for the principal part.

The collision term consists of two separate contributions $C_R$ and $C_I$, arising from the imaginary parts of $(\omega-\mathbf{k}\cdot\mathbf{v}+i0)^{-1}$ and $G(k,\omega)$, respectively. If we set $G(k,\omega)=0$, Eq. (39) reduces to the Balescu-Guernsey-Lenard collision term.[27] Since the DLFC, Eq. (22), approaches unity in the limit of large $k$ and at any finite $\omega$, the $k$ integrations in Eqs. (40) and (41) are convergent in the large-$k$ domain; in the small-$k$ domain they are likewise convergent owing to the dielectric screening.[27] The collision term Eq. (39) thus unifies the treatments of the long- and short-range Coulomb collisions automatically.[31]

It can be proved that the particle number and the mean momentum are conserved in this kinetic equation; by its construction[9] the internal energy is also conserved. Because the present collision term takes account of the frequency dependence in the local-field correction, which was neglected in the static approximation of the earlier

theory,[31] it is applicable not only to the weakly coupled plasmas but also to those strongly coupled plasmas where the interparticle correlations play an essential part.

For the calculation of the coefficient of shear viscosity $\eta$, we follow the procedure described in Ref. 31. We consider a stationary plasma with a flow velocity $\mathbf{u}(z)$, a function of $z$ alone, in the direction of the $x$ axis; the collision term (39) thus becomes a function of the peculiar velocity $\mathbf{w}=\mathbf{v}-\mathbf{u}(z)$. The solution to the kinetic equation is now expressed in a form that the inverse $1/\eta$ of the shear viscosity is written as a sum of the contributions arising from $C_R$ and $C_I$,

$$\frac{1}{\eta}=\frac{1}{\eta_R}+\frac{1}{\eta_I} . \tag{42}$$

The term $1/\eta_R$ is calculated in the same way as that described in Ref. 31. The result is

$$\frac{1}{\eta_R^*}=\frac{12\sqrt{3}}{5\pi}\Gamma^{5/2} \times\int_0^\infty \frac{dx}{x}\int_0^\infty dz \frac{1-\mathrm{Re}G(x/a,\omega_0 xz)}{|\tilde{\epsilon}(x/a,\omega_0 xz)|^2}\exp(-z^2) \tag{43}$$

with $\omega_0=(k_BT/m)^{1/2}/a$. Here we have introduced a dimensionless shear viscosity[1] via

$$\eta^*\equiv\eta/mn\omega_p a^2 . \tag{44}$$

To obtain an expression for $1/\eta_I$, we make use of the formulas

$$\overline{k_x w_z}+\overline{k_z w_x}=0 , \tag{45}$$

$$\overline{(k_x w_z+k_z w_x)^2}=k^2w^2(3+\cos^2\alpha)/15 , \tag{46}$$

$$\overline{(k_x w_z+k_z w_x)(k_x w_z'+k_z w_x')}=\tfrac{4}{15}k^2 ww'\cos\alpha\cos\alpha' , \tag{47}$$

and

$$\overline{(k_x w_z+k_z w_x)(w_x w_z+w_x' w_z')} =\tfrac{1}{30}kw\cos(\alpha)[w^2(4\cos^2\alpha+3\sin^2\alpha) +2w'^2(2\cos^2\alpha'-\sin^2\alpha')] , \tag{48}$$

where the upper bar and $\alpha$ (or $\alpha'$) denote the angular averaging with respect to the rotation of the $xyz$ coordinate system and the angle between $\mathbf{k}$ and $\mathbf{w}$ (or $\mathbf{w}'$), respectively. We thus find

$$\frac{1}{\eta_I^*}=\frac{\sqrt{3}}{5\pi^2}\Gamma^{5/2}\int_0^\infty\frac{dx}{x}\int_{-\infty}^\infty dy\int_{-\infty}^\infty dz\frac{1}{y-z}\left[(2z^2-2yz+3)\frac{\mathrm{Im}G(x/a,\omega_0 xy)}{|\tilde{\epsilon}(x/a,\omega_0 xy)|^2}-(2y^2-2yz+3)\frac{\mathrm{Im}G(x/a,\omega_0 xz)}{|\tilde{\epsilon}(x/a,\omega_0 xz)|^2}\right] \times\exp\left[-\frac{y^2+z^2}{2}\right] . \tag{49}$$

The expression for $G(k,\omega)$ as expressed in Eqs. (22) and (25) contains $\eta$. Hence Eq. (42) together with Eqs. (43) and (49) constitutes a self-consistent equation for $\eta$. Once the static correlation functions and the equation of state for the OCP are given, $\eta$ and $G(k,\omega)$ can be determined simultaneously through a solution to Eq. (42).

## V. DYNAMIC PROPERTIES

In this section we carry out numerical calculations of the shear viscosity, the self-diffusion coefficient, and the dynamic structure factor for the strongly coupled OCP, both in the ordinary fluid phase ($\Gamma<\Gamma_m$) and in the supercooled fluid phase ($\Gamma>\Gamma_m$), on the basis of the dynamic theory developed in the preceding sections. We thereby explore the possibility of a dynamic glass transition in the OCP through the variation of $\eta^*$. In the calculations we use the functional values of the static structure factors obtained in the IHNC scheme, and the equation of state derived through extrapolation of the fluid-state formula due to Slattery, Doolen, and DeWitt.[3]

### A. Shear viscosity

In solving Eqs. (42), (43), and (49) for $\eta^*$ iteratively, we first adopt the Gaussian form, Eq. (27), for the relaxation time $\tau_m(k)$, Eq. (26). The free parameter has been chosen at $\xi_G=2.7$, so that the computed results of $\eta^*$ closely reproduce the MD values[1,5] for $\Gamma\leq 100$. In Table I we list the values of $\eta^*$ computed with $\xi_G=2.6$, 2.7, and 2.8 at $\Gamma=1$, 10, and 100, together with the MD results. We remark that the calculated values of $\eta^*$ appear to be sensitive quantitatively to the choice of $\xi_G$ for $\Gamma\gtrsim 100$. The calculation scheme in the Gaussian approximation with $\xi_G=2.7$ is hereafter referred to as scheme I.

In the static approximation to the local-field correction, $G(k,\omega)\simeq G(k)$, no free parameters are involved in the calculations of $\eta^*$. We found in Ref. 31 that the results of the static approximation showed a fair agreement with the theoretical values of Vieillefosse and Hansen[28] and of Wallenborn and Baus[33] as well as the MD values for

TABLE I. Values of $\eta^*$ calculated in the Gaussian approximation, Eq. (27), with $\xi_G=2.6$, 2.7, and 2.8. The MD values are taken from Ref. 5.

| $\Gamma$ | MD | $\xi_G=2.6$ | $\xi_G=2.7$ | $\xi_G=2.8$ |
|---|---|---|---|---|
| 1 | 1.040±0.21 | 1.14 | 1.12 | 1.10 |
| 10 | 0.085±0.017 | 0.0639 | 0.0614 | 0.0590 |
| 100 | 0.18 ±0.03 | 0.265 | 0.210 | 0.170 |

TABLE II. The reduced shear viscosity $\eta^*$ calculated in scheme I. IHNC refers to the calculations in which the static structure factors are computed in the IHNC scheme; HNC, in the HNC scheme; WB, the values based on the formula proposed by Wallenborn and Baus (Ref. 33).

| $\Gamma$ | IHNC | HNC | WB |
|---|---|---|---|
| 160 | 0.303 | | 0.287 |
| 200 | 0.352 | | 0.338 |
| 300 | 0.456 | 0.279 | 0.489 |
| 400 | 0.553 | | 0.673 |
| 500 | 0.691 | 0.385 | 0.937 |
| 600 | 0.873 | | 1.26 |
| 700 | 1.17 | | 1.69 |
| 800 | 1.81 | | 2.27 |
| 900 | 5.89 | | 3.10 |
| 1000 | 15.8 | 0.798 | 4.32 |
| 1200 | | 1.24 | |
| 1300 | | 1.88 | |
| 1320 | | 5.00 | |
| 1350 | | 15.6 | |
| 1400 | | 19.7 | |
| 1500 | | 26.2 | |
| 1600 | | 31.9 | |
| 1700 | | 37.2 | |
| 1800 | | 42.1 | |

$\Gamma \lesssim 20$. We also observed a small but systematic overestimation of $\eta^*$ as compared with those theoretical or MD values and a divergence of $\eta^*$ value to infinity at $\Gamma \simeq 30$ in the static approximation; these difficulties have been erased in the present calculation due to the inclusion of the frequency dependence and in particular the imaginary part of the local-field correction $G(k,\omega)$. In the weak-coupling limit ($\Gamma \ll 1$), however, both the values in the DLFC and SLFC schemes asymptotically approach those values obtained on the basis of the Landau[34] and the Balescu-Guernsey-Lenard[35] collision terms.

To investigate the variation of $\eta^*$ in the supercooled phase, we have calculated the values of $\eta^*$ in scheme I for $\Gamma \geq 160$; the results are shown in Table II and Fig. 4. For comparison we also exhibit in the table the values of $\eta^*$ obtained by using the static structure factor calculated in the HNC approximation[1,2] and those computed on the basis of the formula proposed by Wallenborn and Baus[33] (WB). Apparently we observe in Fig. 4 a steep rise in the values of $\eta^*$ at $\Gamma = 800-1000$ by a factor of approximately 10 in the present calculation.

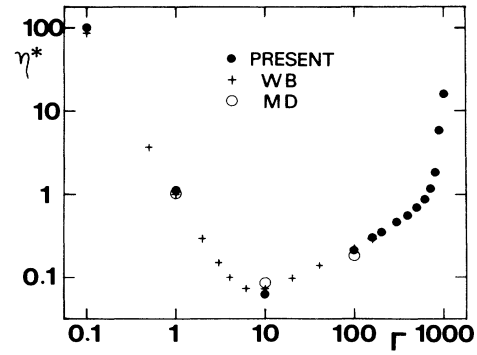


FIG. 4. Reduced shear viscosity $\eta^*$ calculated in various schemes. Solid circles refer to the results in scheme I; crosses, the calculation by Wallenborn and Baus (Ref. 33); open circles, the MD result (Ref. 5).

Although the solution $\eta^*$ itself is quite sensitive quantitatively to the forms of $Y(k)$ and $S(k)$, the qualitative features that the value of $\eta^*$ increases steeply at around $\Gamma \simeq 1000$ appears to be invariable regardless of the computational details. We thus interpret that steep rise of $\eta^*$ at $\Gamma \simeq 800-1000$ observed in Fig. 4 as indication of a dynamic glass transition in the OCP system; this point will be elucidated in the analyses of the dynamic properties in the following. We also remark that the features of the glass transition in the present theory may not be exactly the same as those in the simplified model proposed by Leutheusser *et al.*,[17-19] where it was shown that the state with diverging viscosity and vanishing diffusivity could be obtained mathematically.

### B. Self-diffusion coefficient

Although the information on the single-particle motions is in general necessary[4,36,37] for a calculation of the self-diffusion coefficient $D$, we here undertake its evaluation without that information by evoking the correspondence[2] between a strongly coupled OCP and a HS system. On the basis of the Gibbs-Bogoliubov inequalities for the free energy,[2] DeWitt and Rosenfeld[20] performed a variational calculation of the equation of state for the OCP in which the HS system with radius $\rho$ was chosen as a reference system; they thereby found a correspondence applicable for $\Gamma \gg 1$,

$$\Gamma = 2\frac{\rho}{a}\frac{[1+2(\rho/a)^3]^2}{[1-(\rho/a)^3]^4} . \tag{50}$$

The OCP system with a given value of $\Gamma$ may thus be looked upon as an effective HS system with a packing fraction $(\rho/a)^3$ determined via Eq. (50). The reduced self-diffusion coefficient is then calculated from $\eta^*$ by evoking the Stokes-Einstein relation[21] as

$$D^* \equiv \frac{D}{\omega_p a^2} = \frac{2}{27(\rho/a)\Gamma\eta^*} . \tag{51}$$

Equations (50) and (51) connect $\eta^*$ computed in the preceding section with $D^*$ in the strong-coupling regime. We plot in Fig. 5 the values of $D^*$ calculated on the basis of scheme I. For comparison we also show in the figure the extrapolation of the fitting formula, $D^* = 2.95\Gamma^{-1.34}$, which was obtained on the basis of the MD simulation data[4] at $\Gamma \leq 152.4$. The present evaluations show a fairly good agreement with the MD results for $\Gamma \lesssim 100$. In the supercooled domain, however, the calculated values gradually deviate from the extrapolated line of the MD data. As one would expect, the values of $D^*$ steeply decrease at $\Gamma \simeq 800-1000$ in the present calculation.

### C. Dynamic structure factor

Once the shear viscosity $\eta$ and the relaxation time $\tau_m(k)$ are obtained, we can calculate the dynamic correla-

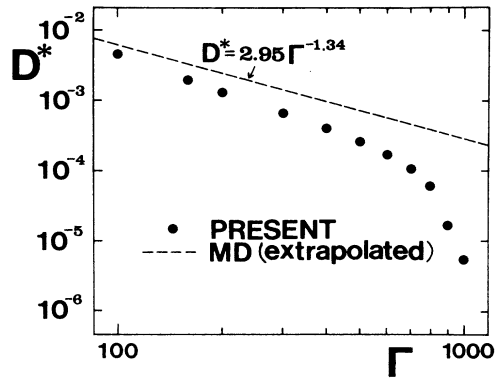


FIG. 5. Reduced self-diffusion coefficient $D^*=D/\omega_p a^2$ calculated in scheme I (solid circles). The dashed line refers to the extrapolation of the fitting formula obtained by the MD simulation (Ref. 4).

tion functions $G(k,\omega)$, $\epsilon(k,\omega)$, and $S(k,\omega)$ through Eqs. (22), (5), and (6). In order to examine the accuracy of the present dynamic theory, we first compare in Figs. 6–9 the calculated values of $S(k,\omega)$ at $\Gamma=160$ with the MD simulation data[4] at $\Gamma=152.4$. As a whole, the present results reproduce the MD data as well as other theoretical calculations[38,39] despite the relatively simple structure adopted for $G(k,\omega)$. We remark that in the static approximation, $G(k,\omega)\simeq G(k)$, one cannot draw the figures for $S(k,\omega)$ in the long-wavelength regime (e.g., at $ak=0.875$ and 1.8562) because of the δ-function-like peak of the plasmon; the present dynamic calculations can well describe the collisional broadening of the plasmon line quantitatively.

We next exhibit in Fig. 10 the results for $S(k,\omega)$ in the scheme I at $\Gamma=500$ and 1000. As the value of $\eta^*$ increases, the central peak (at $\omega=0$) of $S(k,\omega)$ is enhanced remarkably. To see the steep growth in the quasielastic peak of $S(k,\omega)$ as the glassy state is approached, we depict in Fig. 11 the variations of $S(k,0)$ at various values

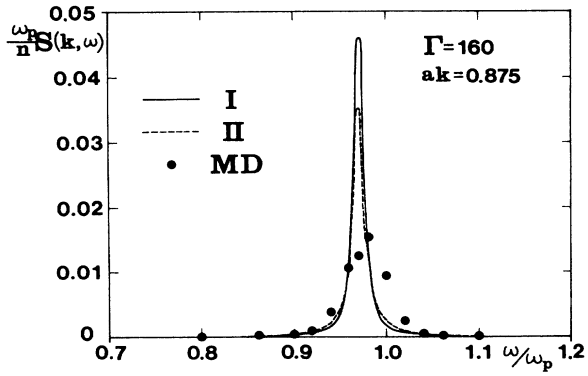


FIG. 6. Normalized dynamic structure factors $(\omega_p/n)S(k,\omega)$ at $\Gamma=160$ for $ak=0.875$. I refers to the calculation in scheme I [Gaussian approximation for $Y(k)$ with $\xi_G=2.7$ and $\eta^*=0.303$]; II, in scheme II [Lorentzian approximation for $Y(k)$ with $\xi_G=1.25$ and $\eta^*=0.281$]. Solid circles represent the results of the MD simulation at $\Gamma=152.4$ (Ref. 4).

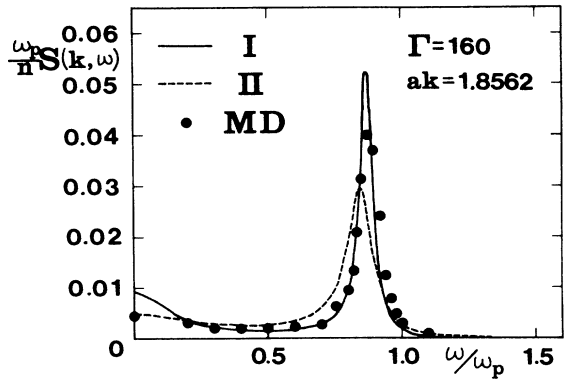


FIG. 7. Same as Fig. 6, but for $ak=1.8562$.

of Γ. The maximum value (at $ak\simeq 4.3$) of $(\omega_p/n)S(k,0)$ at $\Gamma=1000$ is about one thousand times as large as that at $\Gamma=160$.

In Table III we list the plasmon dispersion relation obtained in the calculations of $S(k,\omega)$ at $\Gamma=160$, 500, and 1000. We observe in the table the negative dispersion analogous to that found in the MD simulation[4] in the strong-coupling regime.

The kinetic theory developed in Sec. IV has adopted an approximate truncation scheme, Eq. (32), in the derivation of the collision term, Eqs. (39)–(41). As will be investigated in the Appendix, however, such a truncation procedure has room for a further improvement. We may thus adopt an alternative truncation scheme in which $G(k,\omega)$ in Eq. (32) is replaced by a renormalized function, $G_r(k,\omega)$, as

$$G_r(k,\omega)=\frac{G_r(k)-i\omega\tau_m(k)I(k)}{1-i\omega\tau_m(k)} \tag{52}$$

with

$$G_r(k)=1+\frac{k^2}{k_D^2}-\left[1+\frac{k^2}{k_D^2}-G(k)\right]/\sqrt{A(k)} \tag{53}$$

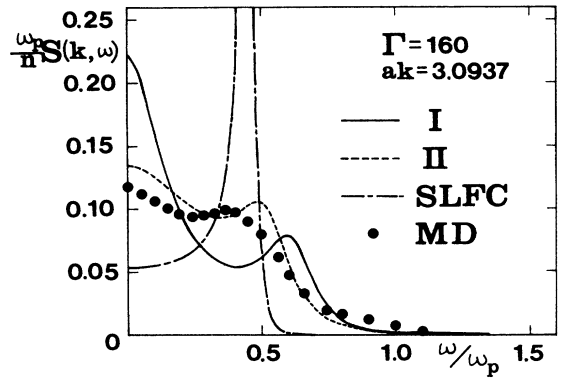


FIG. 8. Same as Fig. 6, but for $ak=3.0937$. SLFC refers to the result in the static approximation for the local-field correction, $G(k,\omega)\simeq G(k)$.

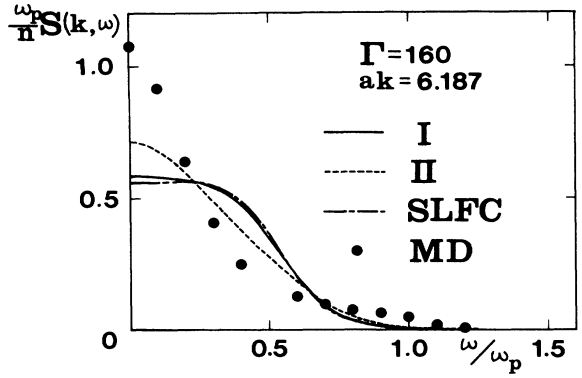


FIG. 9. Same as Fig. 8, but for $ak=6.187$.

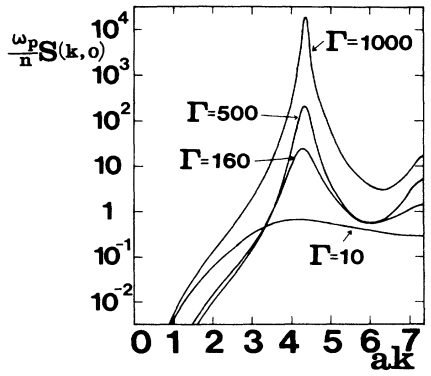


FIG. 11. Values of $(\omega_p/n)S(k,0)$ as functions of the wave number at various values of Γ obtained in scheme I.

and

$$A(k)=1+\left[\frac{2}{\pi}\right]^{1/2}\frac{k_D}{k}\omega_p\tau_m(k)[G(k)-I(k)]\ . \quad (54)$$

Noting also that the Gaussian approximation, Eq. (27), for $Y(k)$ has a tendency of overemphasizing the $k$ dependence (compare between Figs. 8 and 9), we have recalculated $\eta$ and $S(k,\omega)$ on the basis of Eq. (52) coupled with the Lorentzian approximation, Eq. (28), for $Y(k)$ with $\xi_L=1.25$; this calculation scheme is referred to as scheme II. At $\Gamma=160$, we find $\eta^*=0.281$; the results for $S(k,\omega)$ are exhibited in Figs. 6–9 as curves II. We observe in the figures that curves II reproduce the MD results more closely than curves I in the large-$k$ regime.

## VI. POSSIBILITY OF REALIZING AN AMORPHOUS GLASSY STATE

For a realization of the glassy OCP investigated in the preceding sections, a sufficiently rapid quench must be applied to such a plasma, overcoming the nucleation of crystals in the supercooled liquids. In this section we estimate the lifetime of the metastable supercooled state based on a standard statistical model[40,41] of homogeneous nucleation and thereby investigate a relevance of the present theory to laboratory experiments.[10,11]

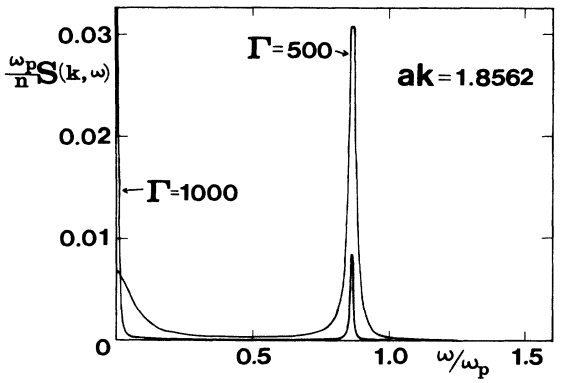


FIG. 10. Normalized dynamic structure factors at $\Gamma=500$ and 1000 for $ak=1.8562$ calculated in scheme I.

The probability of homogeneous nucleation of crystals with radius $r$ is proportional[40] to $\exp[-R_{\min}(r)/k_BT]$, where $R_{\min}(r)$ is the minimum work needed to form the nucleus. Following Turnbull,[41] we may assume that $R_{\min}(r)$ can be expressed as a sum of the surface and bulk terms,

$$R_{\min}(r)\simeq 2k_BT_m(r/a)^2-(\mu_F-\mu_C)(r/a)^3\ , \quad (55)$$

where $T_m$ and $\mu_F-\mu_C$ denote the melting temperature and the free-energy difference per particle between the fluid and crystalline phases. Maximizing $R_{\min}(r)$ with respect to $r$, we have the critical radius of nucleation[12]

$$\frac{r_{cr}}{a}=\frac{4}{3}\frac{k_BT}{\mu_F-\mu_C}\frac{\Gamma}{\Gamma_m} \quad (56)$$

and the minimum work at $r_{cr}$,

$$\frac{R_{\min}(r_{cr})}{k_BT}=\frac{32}{27}\left[\frac{k_BT}{\mu_F-\mu_C}\right]^2\left[\frac{\Gamma}{\Gamma_m}\right]^3 . \quad (57)$$

The diffusion time $t_D$ for a particle to travel over a distance $r_{cr}$ and the mean nucleation time $t_N$ to form crystals are then estimated as

$$\omega_p t_D=\omega_p\frac{r_{cr}^2}{D}=\left[\frac{r_{cr}}{a}\right]^2\frac{1}{D^*} \quad (58)$$

and

$$\omega_p t_N=\omega_p t_D\exp\left[\frac{R_{\min}(r_{cr})}{k_BT}\right] . \quad (59)$$

TABLE III. The plasmon-dispersion relation, $\omega/\omega_p$ as a function of $ak$ at $\Gamma=160$, 500, and 1000 obtained in scheme I.

| $ak$ | $\Gamma=160$ | $\Gamma=500$ | $\Gamma=1000$ |
|---|---|---|---|
| 0.875 | 0.97 | 0.97 | 0.97 |
| 1.8562 | 0.87 | 0.87 | 0.86 |
| 3.0937 | 0.59 | 0.61 | 0.62 |

We have calculated the free energy $\mu_C$ in the crystalline phase from the formula obtained by Slattery, Doolen, and DeWitt.[3] The free energy $\mu_F$ in the supercooled fluid state, $200 \leq \Gamma \leq 1000$, has been calculated in two ways, by extrapolating the formula of Slattery *et al.*[3] and by actually performing for $\Gamma \geq 200$ the coupling-constant integration of the IHNC interaction energies; the results are listed in Table IV.

In Fig. 12 we plot the computed values of the diffusion time and the nucleation time as functions of $\Gamma$. We observe large discrepancies between the solid curves (the IHNC results) and the dashed curves (extrapolation of the MC fluid formula), despite the fact that the free-energy differences have been confined to within 0.15%. To close those gaps, extremely accurate equations of state for both the supercooled fluid and crystalline OCP's would have to be derived, which would call for further developments in the computer-simulation work and the analytic theory. We may nevertheless conclude from Fig. 12 that $\omega_p t_N$ takes on a minimum value somewhere between $10^9$ and $10^{13}$ at $\Gamma \simeq 400$. If the system is quenched faster than the minimum value of $\omega_p t_N$ down to $\Gamma \simeq 1000$, we may be able to realize a glassy OCP.

Recently, Bollinger and Wineland[11] have produced Penning-trapped, strongly coupled ($\Gamma \simeq 5$–$10$) ion plasma by using the laser-cooling technique; they were able to maintain them stably for many hours. The theoretical limit of the $\Gamma$ value has been estimated to be about $10^4$ for a $^9Be^+$ plasma. Their plasma appears to be a candidate of the OCP glass because of the relative smallness of the plasma frequency, which is $\omega_p \simeq 4.4 \times 10^7$ $(n/10^{10}$ $cm^{-3})^{1/2} s^{-1}$ for $^9Be^+$ plasmas. The minimum value of $t_N$ in Fig. 12 then takes on $2 \times (10$–$10^5)$ s at $n = 10^{10}$ $cm^{-3}$. If the cooling can be administered sufficiently fast to overcome the minimum value of $t_N$, then a highly viscous glassy OCP may be realized in the laboratory.

## VIII. CONCLUDING REMARKS AND DISCUSSION

In this paper we have developed a new kinetic theory of dynamic correlations for a strongly coupled, classical OCP within the generalized viscoelastic formalism; the coefficient of shear viscosity $\eta$ and the dynamic structure factor $S(k,\omega)$ have been calculated self-consistently, with the results reproducing the existing MD data for $\Gamma < \Gamma_m$ satisfactorily. An application of the theory to the plasmas in the supercooled fluid state ($\Gamma > \Gamma_m$) has led us to predict steep variations of $\eta$, $S(k,\omega)$, and $D$ at $\Gamma \simeq 1000$, which we interpret as indications of a dynamic glass transition in the OCP. The transition point appears to be definitely greater than that ($\Gamma \simeq 300$–$400$) predicted through analyses of the structural changes in the static correlation functions. We have finally investigated the possibility of realizing a glassy state in the OCP by evaluating the lifetime of a metastable fluid state against a homogeneous nucleation of crystals.

To determine a glass-transition point in the HS system with radius $\rho$ numerically, Bengtzelius, Götze, and Sjölander[18] (BGS) derived a closed nonlinear equation for

$$f(k) \equiv \lim_{t \to \infty} [\langle \delta n(k,t) \delta n^*(k,0) \rangle / nS(k)] \tag{60}$$

on the basis of a mode-coupling theory; it reads

$$\frac{f(k)}{1-f(k)} = \frac{nS(k)}{8\pi^2 k^3} \int_0^\infty dq\, q \int_{|q-k|}^{|q+k|} dl\, l \left[ \frac{q^2-l^2}{2k}[c(q)-c(l)] + \frac{k}{2}[c(q)+c(l)] \right]^2 S(k)S(l)f(q)f(l) , \tag{61}$$

where $c(k) = [S(k)-1]/nS(k)$ is the Fourier transform of the direct correlation function. If the system is in the glassy state, Eq. (61) should have a nonvanishing solution of $f(k)$ besides a trivial solution $f(k) = 0$. Using the Wertheim-Thiele solution[42] for $S(k)$, they found a transition point $(\rho/a)^3 = 0.516$, which appears to be consistent

TABLE IV. Values of the free-energy density in units of $nk_BT$ obtained by the IHNC calculation or from the fitting formula of Slattery *et al.* based on the MC simulation (Ref. 3).

| $\Gamma$ | Liquid (IHNC) | Liquid (MC) | Solid (MC) |
|---|---|---|---|
| 200 | −157.173 | −157.173 | −157.269 |
| 300 | −244.387 | −244.517 | −245.015 |
| 400 | −332.198 | −332.471 | −333.306 |
| 500 | −420.354 | −420.773 | −421.891 |
| 600 | −508.744 | −509.303 | −510.661 |
| 700 | −597.302 | −597.996 | −599.559 |
| 800 | −685.974 | −686.810 | −688.551 |
| 900 | −774.709 | −775.718 | −777.631 |
| 1000 | −863.432 | −864.703 | −866.731 |

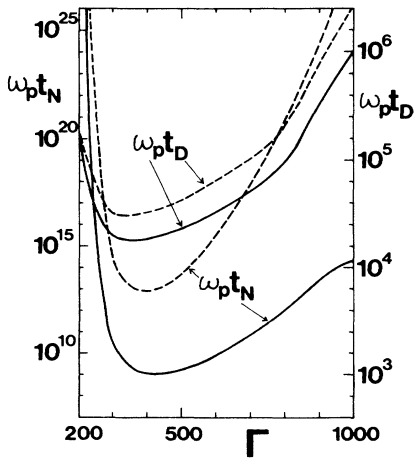


FIG. 12. Reduced diffusion time $\omega_p t_D$ and the reduced nucleation time $\omega_p t_N$. The solid curve refers to the results based on the IHNC free energies; the dashed curves, extrapolation of the fluid formula due to Slattery *et al.* (Ref. 3).

with the computer-simulation values,[43,44] 0.52 or 0.56.

Since the solutions to Eq. (61) are determined only with the knowledge of $S(k)$, we may test their theory in the case of OCP as well. We started the iterative calculations at $\Gamma=1000$ with the initial values of $f(k)=1$; the obtained solutions $f(k)$ were then used as initial values for the iterations at lower values of $\Gamma$. We have thus found nonvanishing solutions of $f(k)$ for $400\leq\Gamma\leq 1000$, two of which are exhibited in Fig. 13. At $\Gamma=300$, however, we have found that the solution crushes to $f(k)=0$; the BGS theory thus predicts that the glass transition takes place somewhere between $\Gamma=300$ and 400 in the OCP system; the critical value of $\Gamma$ is thus smaller substantially than that in the present theory.

In order to obtain more definite predictions on the dynamic properties of the supercooled OCP, further developments in the computer-simulation work and the analytic theory are necessary. The present theoretical estimates may provide a useful guide to design a MD simulation experiment for a glass transition in an OCP system, in a way analogous to one performed recently in a metallic system.[45]

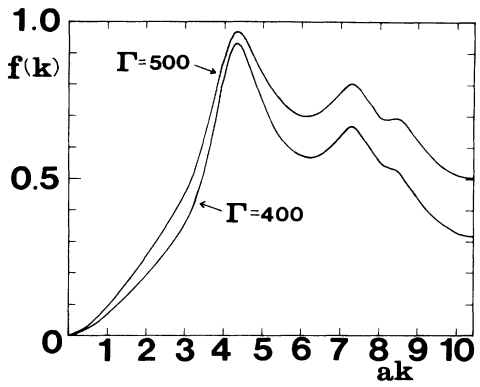


FIG. 13. Values of $f(k)$ obtained as solutions to Eq. (61) at $\Gamma=400$ and 500.

## ACKNOWLEDGMENTS

We wish to thank Dr. H. Iyetomi and A. Nakano for useful discussions on this and related topics. This research was supported in part through a Grant-in-Aid for Scientific Research, No. 59380001, provided by the Japanese Ministry of Education, Science, and Culture. This paper is based in part on the Ph.D. dissertation submitted by S.T. to the Physics Department, University of Tokyo.

## APPENDIX: RENORMALIZATION OF STATIC LOCAL-FIELD CORRECTION

We first replace $G(k,\omega)$ in Eq. (32) by a "renormalized" quantity, $G_r(k,\omega)$. Instead of Eq. (35) we then have

$$\delta n(\mathbf{k},\omega)=\frac{\delta n_0(\mathbf{k},\omega)}{\tilde{\epsilon}_r(\mathbf{k},\omega)}\ , \tag{A1}$$

where

$$\tilde{\epsilon}_r(\mathbf{k},\omega)=1-v(k)[1-G_r(k,\omega)]\chi_0(\mathbf{k},\omega)\ . \tag{A2}$$

Multiplying both sides of Eq. (A1) by their complex conjugates and ensemble averaging the resulting equation in the equilibrium state, we obtain

$$S(k,\omega)=\frac{S_0(k,\omega)}{|\tilde{\epsilon}_r(k,\omega)|^2}\ , \tag{A3}$$

where

$$S_0(k,\omega)=\frac{n}{k}\left[\frac{m}{2\pi k_B T}\right]^{1/2}\exp\left[-\frac{m\omega^2}{2k_B T k^2}\right] \tag{A4}$$

is the dynamic structure factor in the ideal-gas limit. In light of Eqs. (5), (6), and (A3), we find an equation for $G_r(k,\omega)$,

$$\frac{1}{|\tilde{\epsilon}_r(k,\omega)|^2}=\frac{1-v(k)\mathrm{Im}G(k,\omega)|\chi_0(k,\omega)|^2/\mathrm{Im}\chi_0(k,\omega)}{|\tilde{\epsilon}(k,\omega)|^2}\ . \tag{A5}$$

The complex function $G_r(k,\omega)$ is to be so determined that both Eq. (A5) and the Kramers-Kronig relations[27] be satisfied.

If the second term in the numerator on the right-hand side of Eq. (A5) is negligible, we have

$$G_r(k,\omega)=G(k,\omega)\ , \tag{A6}$$

the approximation adopted in Sec. IV. When both $\Gamma$ and $\eta^*$ become large, however, we cannot ignore that term, especially in the low-frequency regime. Taking the limit of $\omega\to 0$, we find from Eq. (A5) such an expression for $G_r(k)\equiv G_r(k,0)$ as Eq. (53). We may thus regard Eq. (53) as a renormalized expression for the SLFC.

Since $A(k)$, Eq. (54), has properties, $A(k)\geq 1$ and $A(0)=A(\infty)=1$, we find

$$G_r(k)\geq G(k)\ , \tag{A7}$$

$$G_r(0)=G(0)=0\ . \tag{A8}$$

and

$$G_r(\infty)=G(\infty)=1\ . \tag{A9}$$

The function $A(k)$ thus enhances the values of the SLFC in the intermediate-wave-number regime. In the static approximation,[31] $G(k,\omega)\simeq G(k)$, one need not renormalize the SLFC because $\tau_m(k)=0$. In the dynamic case, we obtain the renormalized DLFC $G_r(k,\omega)$ simply by replacing $G(k)$ with $G_r(k)$ in Eq. (22); the Kramers-Kronig relations for $G_r(k,\omega)$ are then satisfied automatically.

[1]M. Baus and J.-P. Hansen, Phys. Rep. **59**, 1 (1980).
[2]S. Ichimaru, Rev. Mod. Phys. **54**, 1017 (1982).
[3]S. G. Brush, H. L. Sahlin, and E. Teller, J. Chem. Phys. **45**, 2102 (1966); J.-P. Hansen, Phys. Rev. A **8**, 3096 (1973); W. L. Slattery, G. D. Doolen, and H. E. DeWitt, *ibid.* **21**, 2087 (1980); **26**, 2255 (1982).
[4]J.-P. Hansen, E. L. Pollock, and I. R. McDonald, Phys. Rev. Lett. **32**, 277 (1974); J.-P. Hansen, I. R. McDonald, and E. L. Pollock, Phys. Rev. A **11**, 1025 (1975).
[5]B. Bernu, P. Vieillefosse, and J.-P. Hansen, Phys. Lett. **63A**, 301 (1977); B. Bernu and P. Vieillefosse, Phys. Rev. A **18**, 2345 (1978).
[6]Y. Rosenfeld and N. W. Ashcroft, Phys. Rev. A **20**, 1208 (1979); F. J. Rogers, D. A. Young, H. E. DeWitt, and M. Ross, *ibid.* **28**, 2990 (1983).
[7]H. Iyetomi and S. Ichimaru, Phys. Rev. A **25**, 2434 (1982); **27**, 3241 (1983).
[8]F. J. Rogers and D. A. Young, Phys. Rev. A **30**, 999 (1984).
[9]See, e.g., S. Ichimaru, *Plasma Physics: An Introduction to Statistical Physics of Charged Particles* (Benjamin-Cummings, Menlo Park, 1986).
[10]C. F. Driscoll and J. H. Malmberg, Phys. Rev. Lett. **50**, 167 (1983), and references therein.
[11]J. J. Bollinger and D. J. Wineland, Phys. Rev. Lett. **53**, 348 (1984).
[12]H. Iyetomi and S. Ichimaru, Phys. Rev. A **27**, 1734 (1983); S. Ichimaru, H. Iyetomi, S. Mitake, and N. Itoh, Astrophys. J. Lett. **265**, L83 (1983).
[13]C. A. Angell, J. H. R. Clarke, and L. V. Woodcock, Adv. Chem. Phys. **48**, 397 (1981).
[14]D. Frenkel and J. P. McTague, Annu. Rev. Phys. Chem. **31**, 491 (1980).
[15]J. J. Ullo and S. Yip, Phys. Rev. Lett. **54**, 1509 (1985).
[16]B. Bernu, Y. Hiwatari, and J.-P. Hansen, J. Phys. C **18**, L371 (1985).
[17]E. Leutheusser, Phys. Rev. A **29**, 2765 (1984); Z. Phys. B **55**, 235 (1984); T. R. Kirkpatrick, Phys. Rev. A **31**, 939 (1985).
[18]U. Bengtzelius, W. Götze, and A. Sjölander, J. Phys. C **17**, 5915 (1984); U. Bengtzelius and L. Sjögren, J. Chem. Phys. **84**, 1744 (1986); U. Bengtzelius, Phys. Rev. A **33**, 3433 (1986).
[19]S. P. Das, G. F. Mazenko, S. Ramaswamy, and J. J. Toner, Phys. Rev. Lett. **54**, 118 (1985); S. P. Das and G. F. Mazenko, Phys. Rev. A **34**, 2265 (1986).
[20]H. E. DeWitt and Y. Rosenfeld, Phys. Lett. **75A**, 79 (1979).
[21]S. Nagano and S. Ichimaru, J. Phys. Soc. Jpn. **49**, 1260 (1980).
[22]J. Frenkel, *Kinetic Theory of Liquids* (Clarendon, Oxford, 1946), Chap. IV.
[23]S. Ichimaru and S. Tanaka, Phys. Rev. Lett. **56**, 2815 (1986).
[24]H. R. Wendt and F. F. Abraham, Phys. Rev. Lett. **41**, 1244 (1978).
[25]S. Ichimaru and K. Tago, J. Phys. Soc. Jpn. **50**, 409 (1981).
[26]S. Ichimaru, S. Mitake, S. Tanaka, and X.-Z. Yan, Phys. Rev. A **32**, 1768 (1985).
[27]See, e.g., S. Ichimaru, *Basic Principles of Plasma Physics* (Benjamin, Reading, Mass., 1973).
[28]P. Vieillefosse and J.-P. Hansen, Phys. Rev. A **12**, 1106 (1975).
[29]G. Mukhopadyay and A. Sjölander, Phys. Rev. B **17**, 3589 (1978).
[30]S. Ichimaru, Phys. Rev. A **15**, 744 (1977).
[31]S. Tanaka and S. Ichimaru, Phys. Rev. A **34**, 4163 (1986).
[32]D. Pines, in *Quantum Fluids,* edited by D. F. Brewer (North-Holland, Amsterdam, 1966), p. 257.
[33]J. Wallenborn and M. Baus, Phys. Rev. A **18**, 1737 (1978).
[34]S. I. Braginskii, J. Exp. Theoret. Phys. **33**, 459 (1957) [Sov. Phys.—JETP **6**, 358 (1958)].
[35]E. Braun, Phys. Fluids **10**, 731 (1967).
[36]H. Gould and G. F. Mazenko, Phys. Rev. A **15**, 1274 (1977).
[37]S. Sjödin and S. K. Mitra, J. Phys. A **10**, L163 (1977); S. K. Mitra and S. Sjödin, J. Phys. C **11**, 2655 (1978).
[38]J. Bosse and K. Kubo, Phys. Rev. A **18**, 2337 (1978).
[39]R. Cauble and J. J. Duderstadt, Phys. Rev. A **23**, 3182 (1981).
[40]L. D. Landau and E. M. Lifshitz, *Statistical Physics* (Pergamon, Oxford, 1969), p. 471.
[41]D. Turnbull, J. Appl. Phys. **21**, 1022 (1950).
[42]See, e.g., J.-P. Hansen and I. R. McDonald, *Theory of Simple Liquids* (Academic, New York, 1976).
[43]L. V. Woodcock, J. Chem. Soc. Faraday Trans. 2 **73**, 11 (1977).
[44]L. V. Woodcock and C. A. Angell, Phys. Rev. Lett. **47**, 1129 (1981).
[45]R. N. Barnett, C. L. Cleveland, and U. Landman, Phys. Rev. Lett. **55**, 2035 (1985).